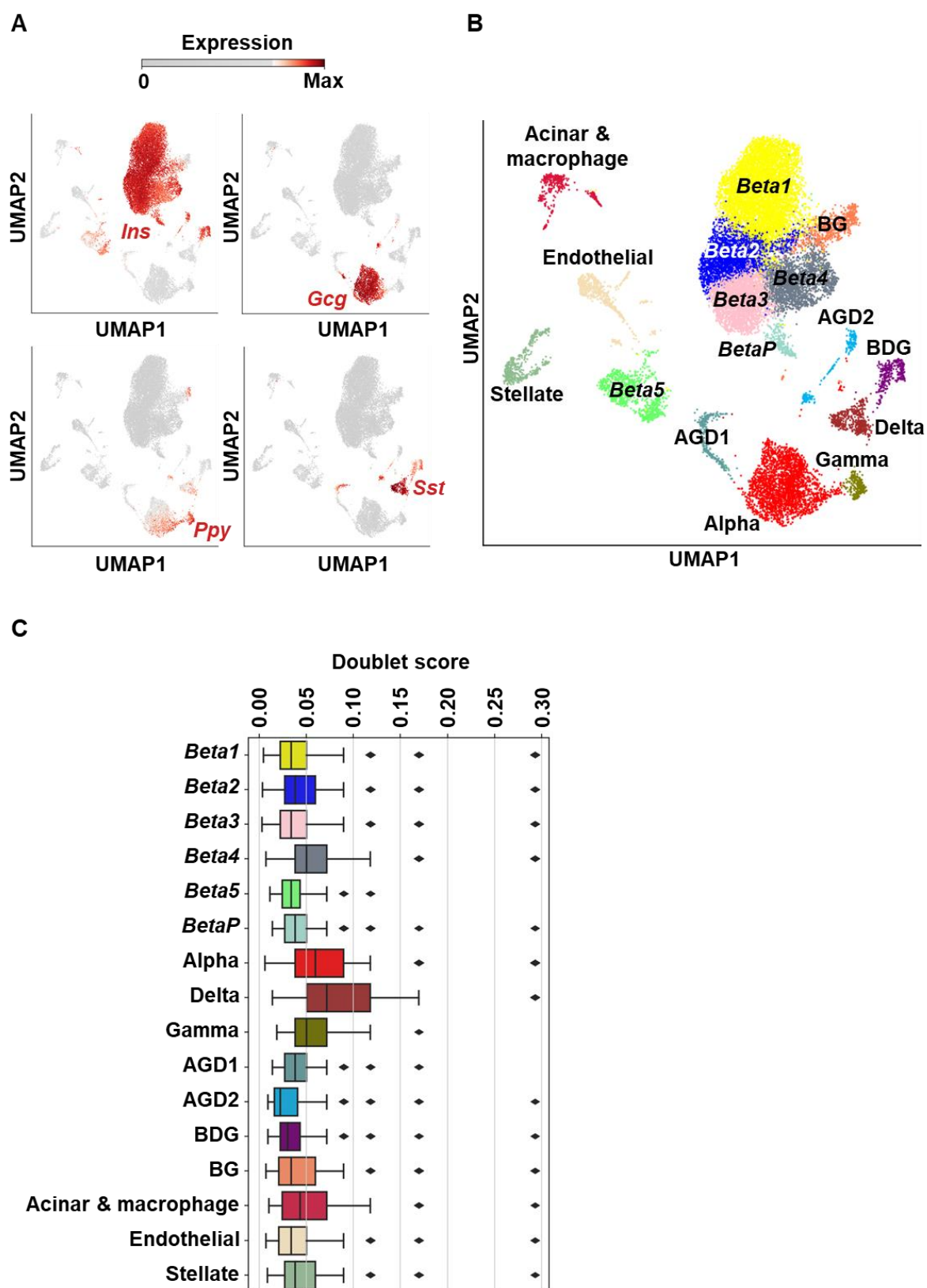
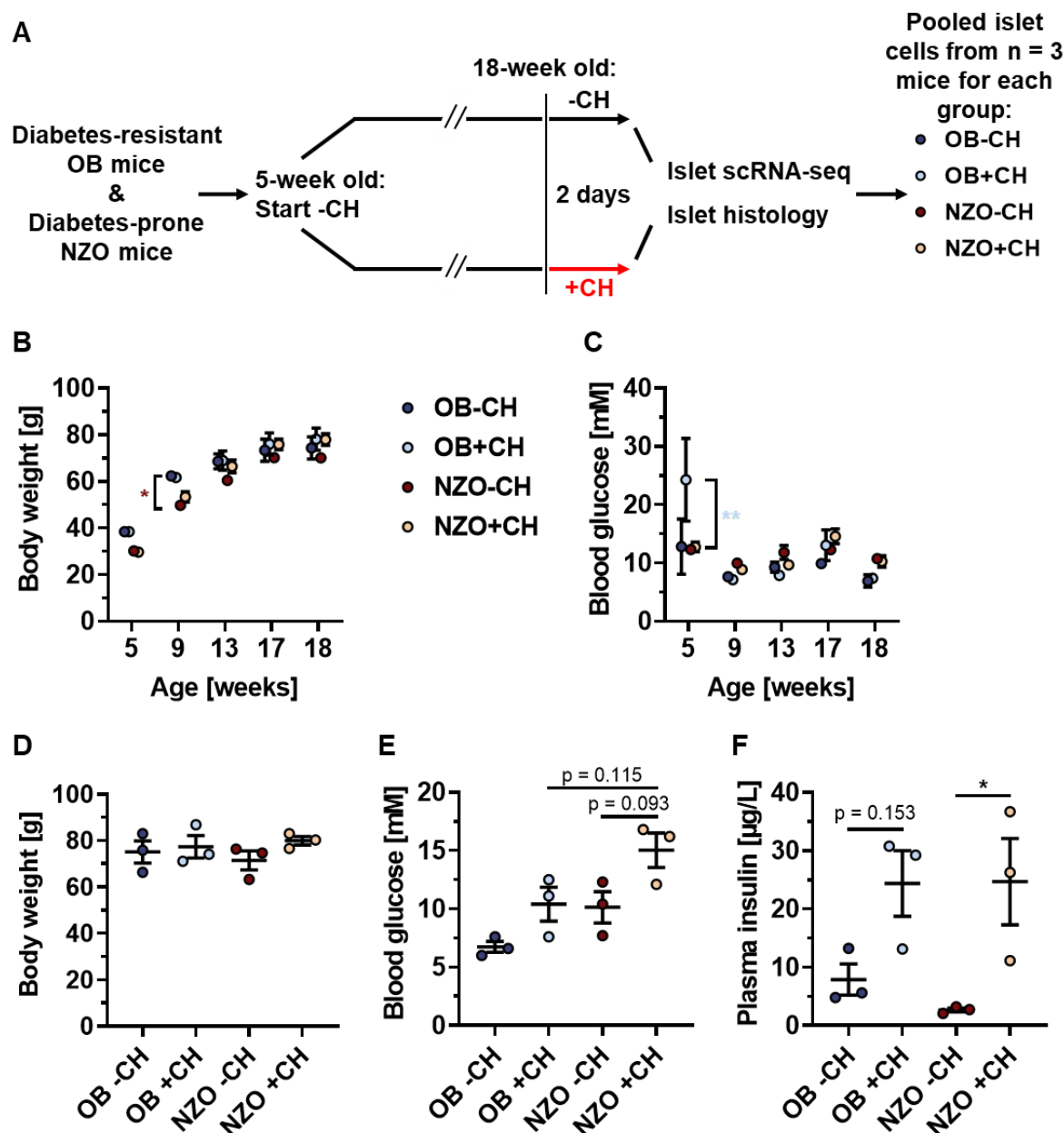


## Online Supplemental Material



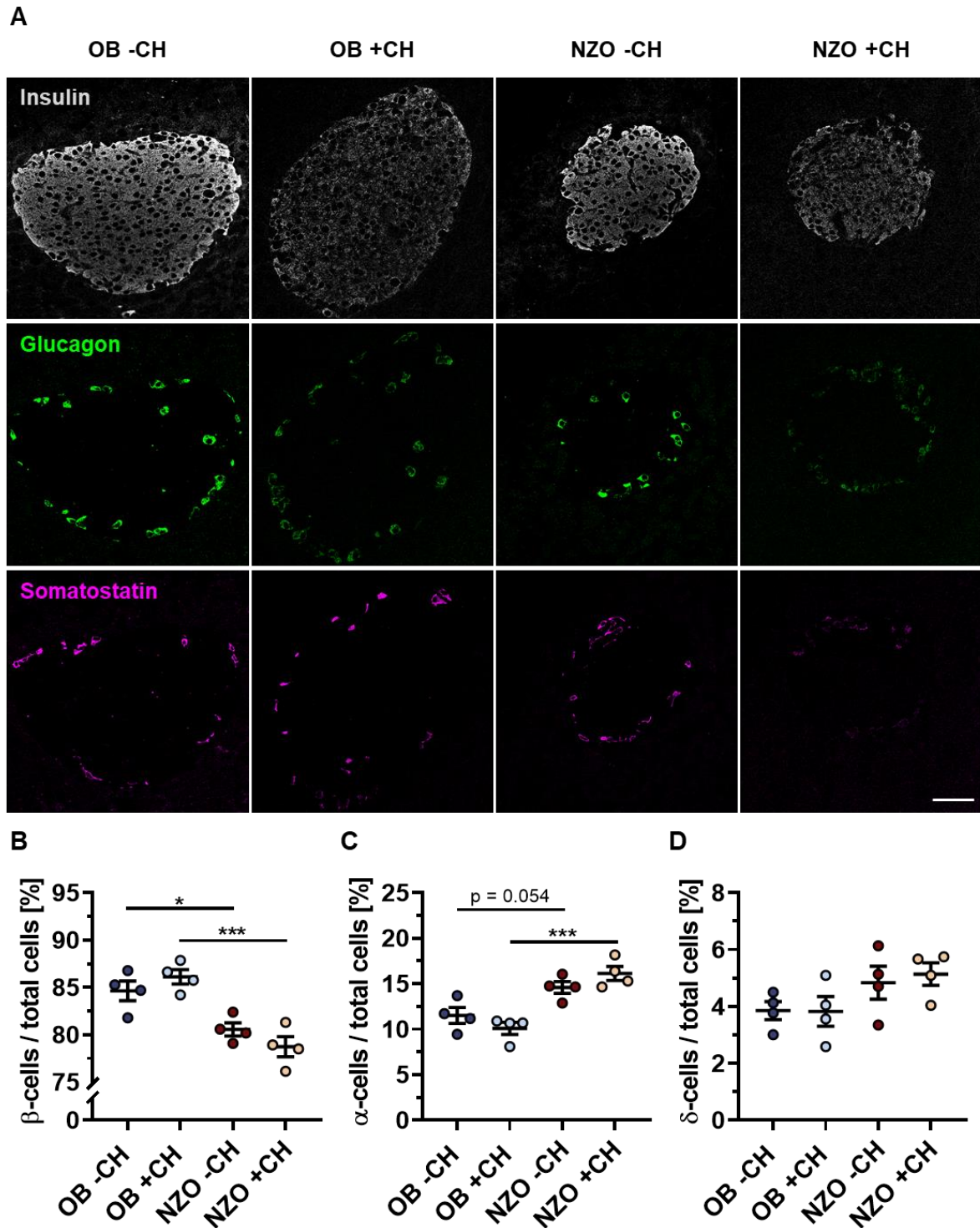
**Supplemental Figure 1. Method of doublet detection and exclusion.**

(A, B) UMAP plot showing the expression of islet cell hormones in single cells (A), compared with cell cluster identification (B). (C) Estimation of doublet cell scores for single cells after removal of previously identified doublets.



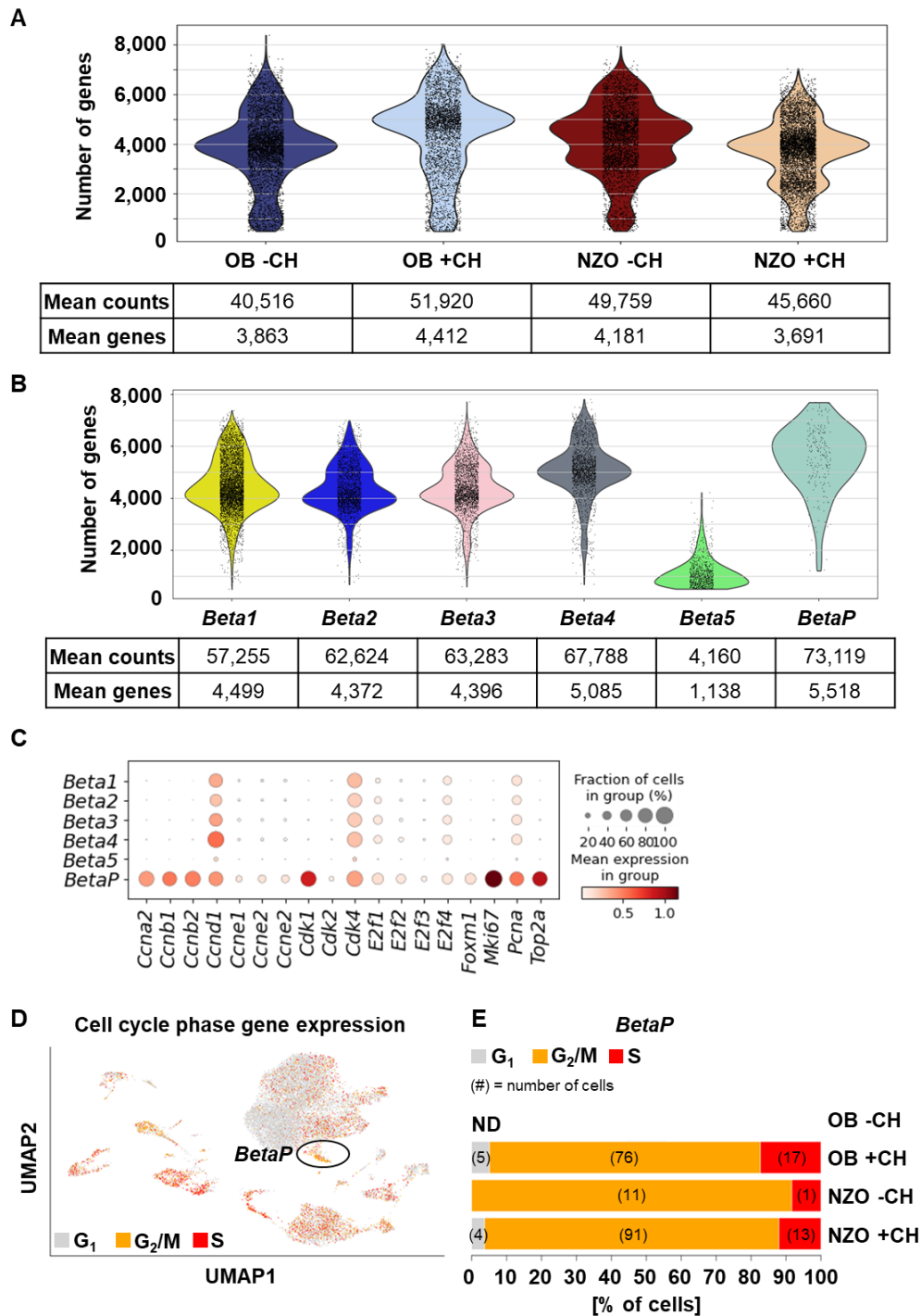
**Supplemental Figure 2. Body weight, blood glucose and plasma insulin levels of OB and NZO mice used for scRNA-seq analysis.**

(A) Depiction of experimental setup. From 5 to 18 weeks of age, male OB and NZO mice were fed carbohydrate-free high-fat diet (-CH). They were then subdivided into two groups fed either -CH or a diabetogenic, carbohydrate-containing high-fat diet (+CH) for two additional days before islet isolation. (B, C) Body weights (B) and blood glucose levels (C) of -CH-fed OB and NZO animals between 5 and 18 weeks of age. (D-F) Body weights (D), blood glucose (E) and plasma insulin levels (F) of 18-week old OB and NZO mice fed -CH or +CH for two additional days. Data are presented as mean  $\pm$  SEM, n = 3, \*  $p < 0.05$  by two-way ANOVA with Tukey's multiple comparisons test.



**Supplemental Figure 3. Differences in endocrine islet cell composition of diabetes-resistant OB and diabetes-prone NZO mice.**

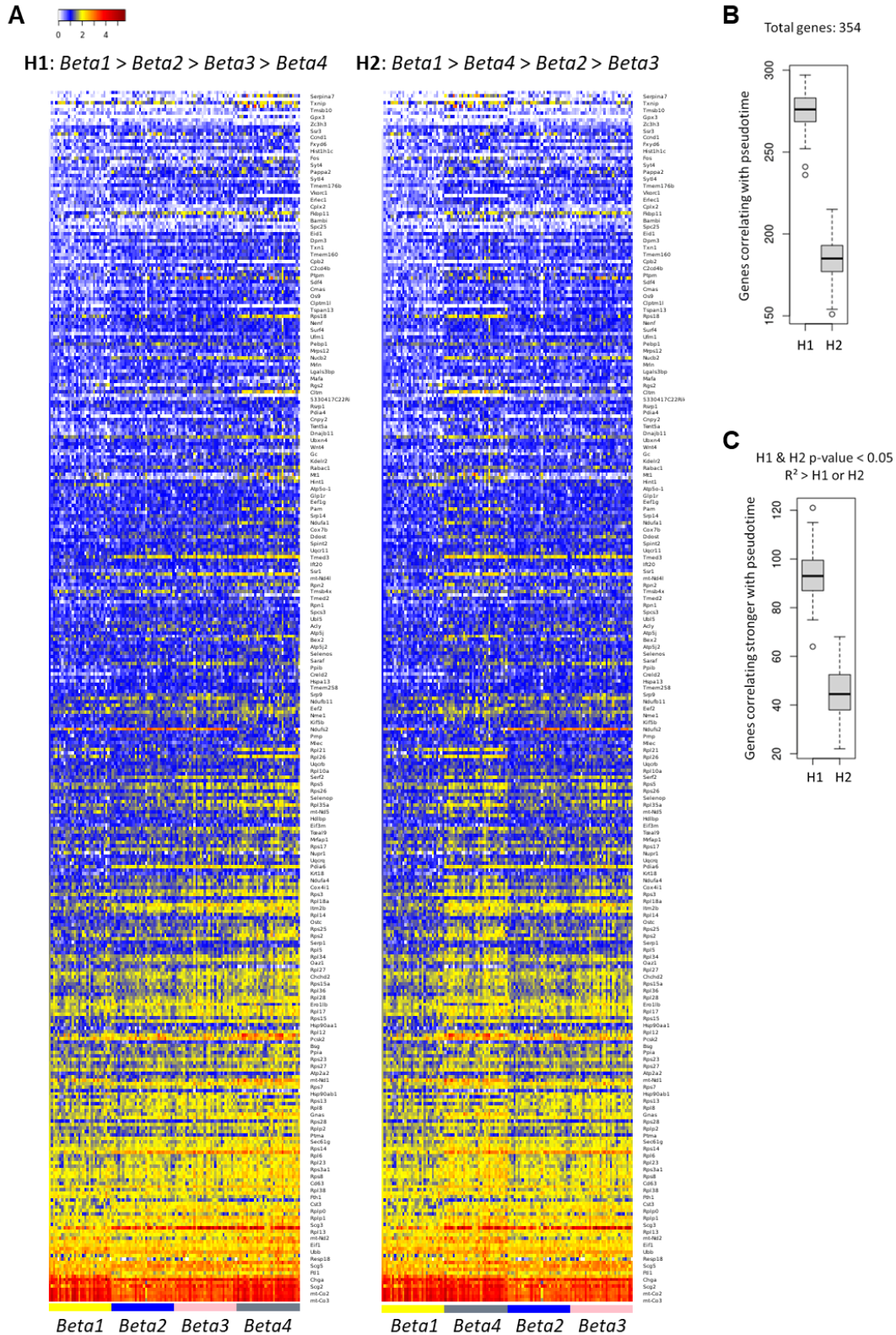
(A) Pancreatic sections of 18-week old OB and NZO mice fed -CH or +CH diet for two days were co-stained for insulin (gray,  $\beta$ -cells), glucagon (green,  $\alpha$ -cells), and somatostatin (magenta,  $\delta$ -cells). Representative images of  $n = 3$ . Scale bar, 50  $\mu$ m. (B-D) Quantification of  $\beta$ -cell (B),  $\alpha$ -cell (C), and  $\delta$ -cell (D) percentage per total number of islet nuclei. Data are represented as mean  $\pm$  SEM,  $n = 4$ , \*  $p < 0.05$ , \*\*\*  $p < 0.001$  by two-way ANOVA with Tukey's multiple comparisons test.



**Supplemental Figure 4. Average number of expressed genes per experimental condition and  $\beta$ -cell clusters of OB and NZO mice with further characterization of proliferative  $\beta$ -cell clusters.**

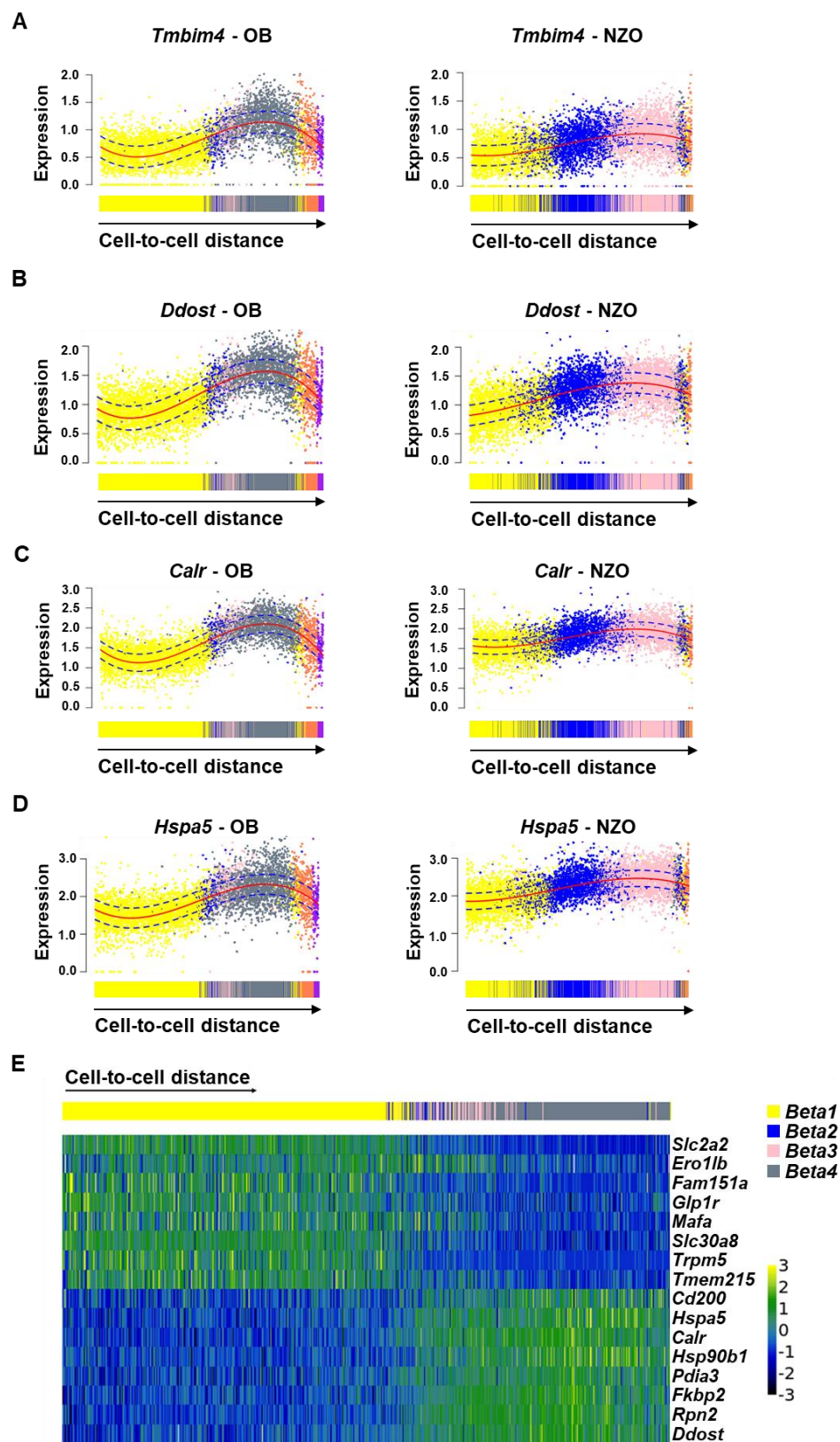
(A, B) The kernel density estimate fit displays the distribution of the number of expressed genes in islet cells from the four indicated experimental groups (A) or in the six  $\beta$ -cell clusters found in OB and NZO islets (B). Each black dot represents data from one single cell. The violin interior depicts median, quartile and whisker values. (C) Dot plot representing the number of cells (dot size) and mean gene expression levels in the *Beta1* to *BetaP* clusters. The proliferative  $\beta$ -cell cluster *BetaP* was identified based on expression of the proliferation marker gene *Mki67* and others. (D) UMAP plot showing the expression of genes annotated to the cell cycle in OB and NZO islet cells. The colour code indicates classification of genes by cell cycle phase (G<sub>1</sub>-phase = gray; G<sub>2</sub>/M-phase = orange; S-phase = red). (E) Quantification of *BetaP* cell cycle phase gene expression signature in the four experimental groups. Absolute numbers of cells are shown in brackets inside the respective bars. In OB -CH islets, no *BetaP* cells were detected (ND).





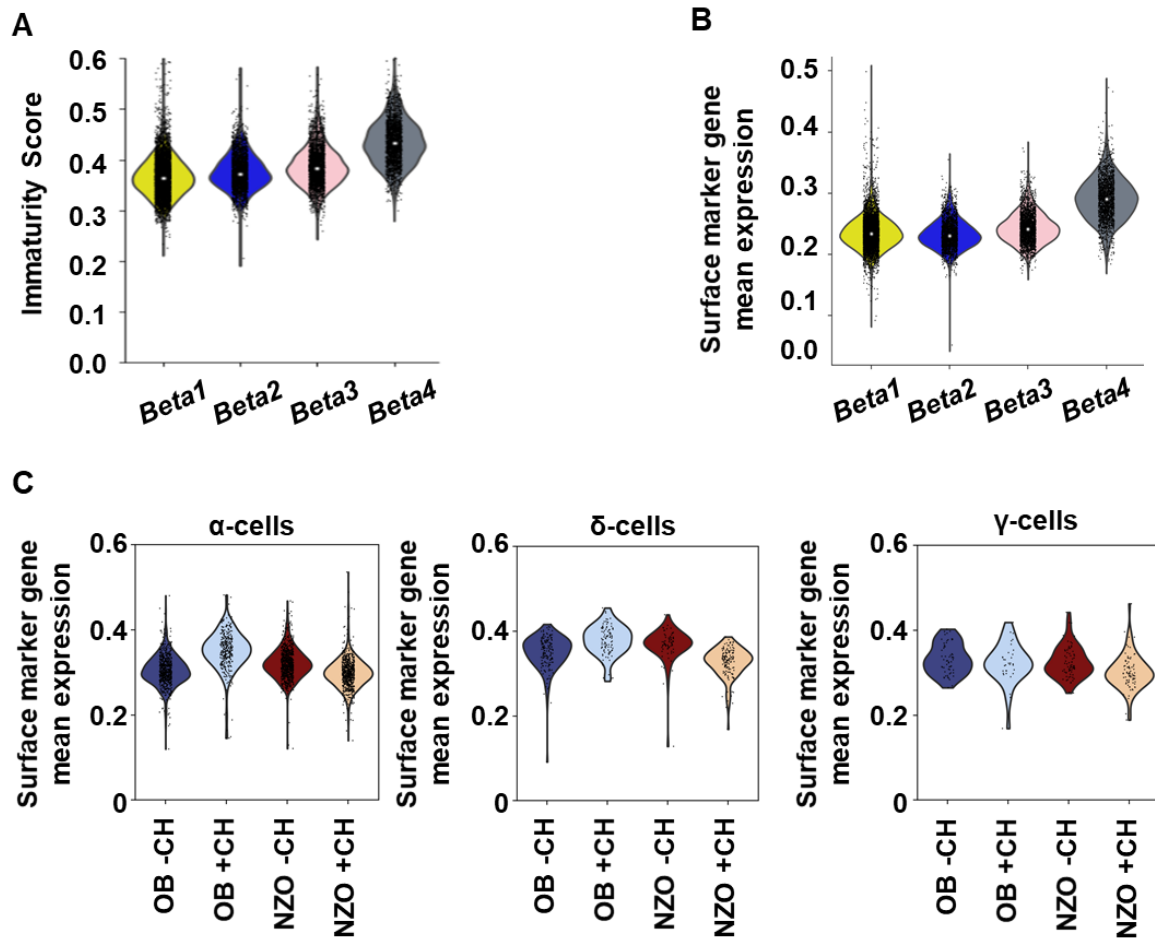
**Supplemental Figure 5. Identification of the most likely  $\beta$ -cell pseudotime lineage.**

(A) Representative heatmaps of differentially expressed genes (DEGs) in 30 randomly selected  $\beta$ -cells from clusters *Beta1-4*. Intra-cluster pre-sorting was achieved via 15 randomly selected, low or high expressed DEGs from the *Beta1* vs. *Beta4* comparison. Two hypotheses (H1, H2) for possible pseudotime lineages were tested. Order of genes (top to bottom) is by expression in *Beta1* (low to high). (B) The process in (A) was repeated 1000 times and the total number of genes correlating significantly with pseudotime H1 or H2 was calculated. (C) Of the genes correlating significantly with H1 or H2, trajectory H1 contains more genes with a high correlation coefficient ( $R^2$ ).



**Supplemental Figure 6. Gene expression changes along the principal OB and NZO  $\beta$ -cell trajectories.**

(A-D) Expression of the anti-apoptotic factor *Tmbim4* (A), OST complex subunit *Ddost* (B), and chaperones *Calr* (C) and *Hspa5* (D) in OB versus NZO  $\beta$ -cells along the inferred trajectory. Dots represent scaled expression levels of individual  $\beta$ -cells, colour-coded according to their cluster allocation. Solid red lines depict fitted curves and dotted blue lines depict confidence intervals. (E) Topmost up- or downregulated genes along the *Beta1* to *Beta4* trajectory.

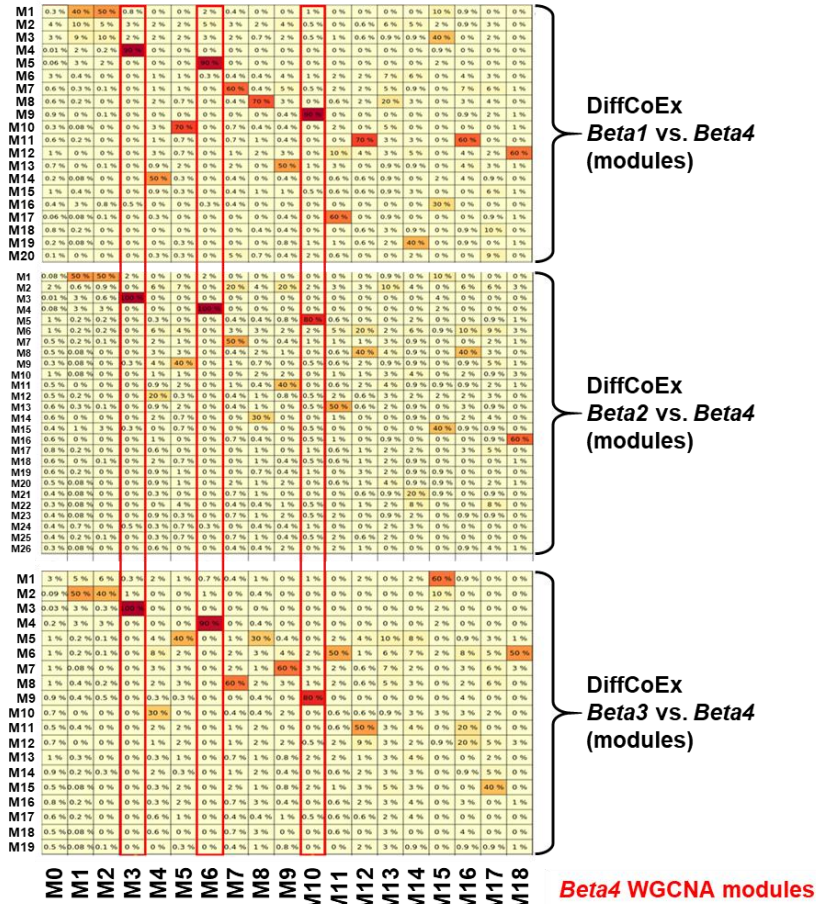


**Supplemental Figure 7. Immaturity score and cell surface marker gene expression**

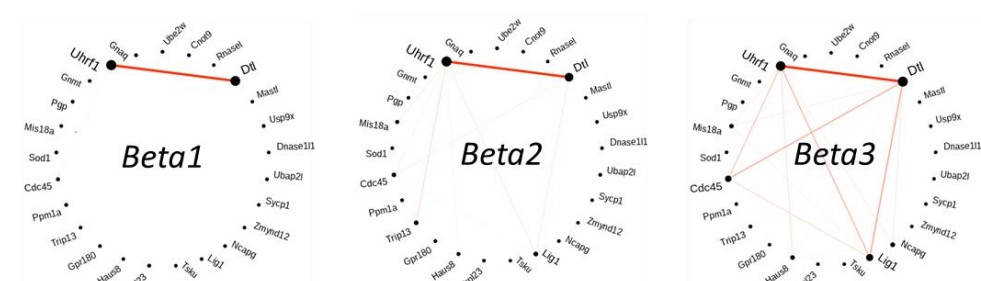
(A) Distribution of  $\beta$ -cell immaturity scores for  $\beta$ -cell clusters *Beta1-4*. Cell scores were calculated by comparing  $\beta$ -cell expression profiles to an independent data set of  $\beta$ -cells during embryonic (E17.5 to P0) to postnatal (P60) development. Black dots indicate the individual scores per single cell. (B) Mean surface marker gene expression per single cell of  $\beta$ -cell clusters *Beta1-4*. (C) Mean surface marker gene expression per single cell separated into monohormonal ( $\alpha$ -,  $\delta$ -,  $\gamma$ -) cells and sorted by experimental groups.



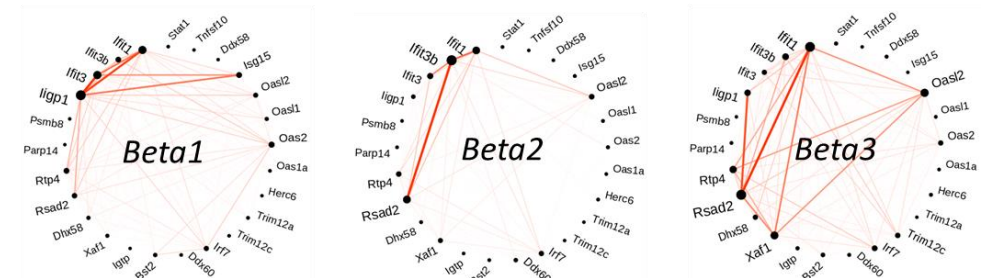
**A**



**B**



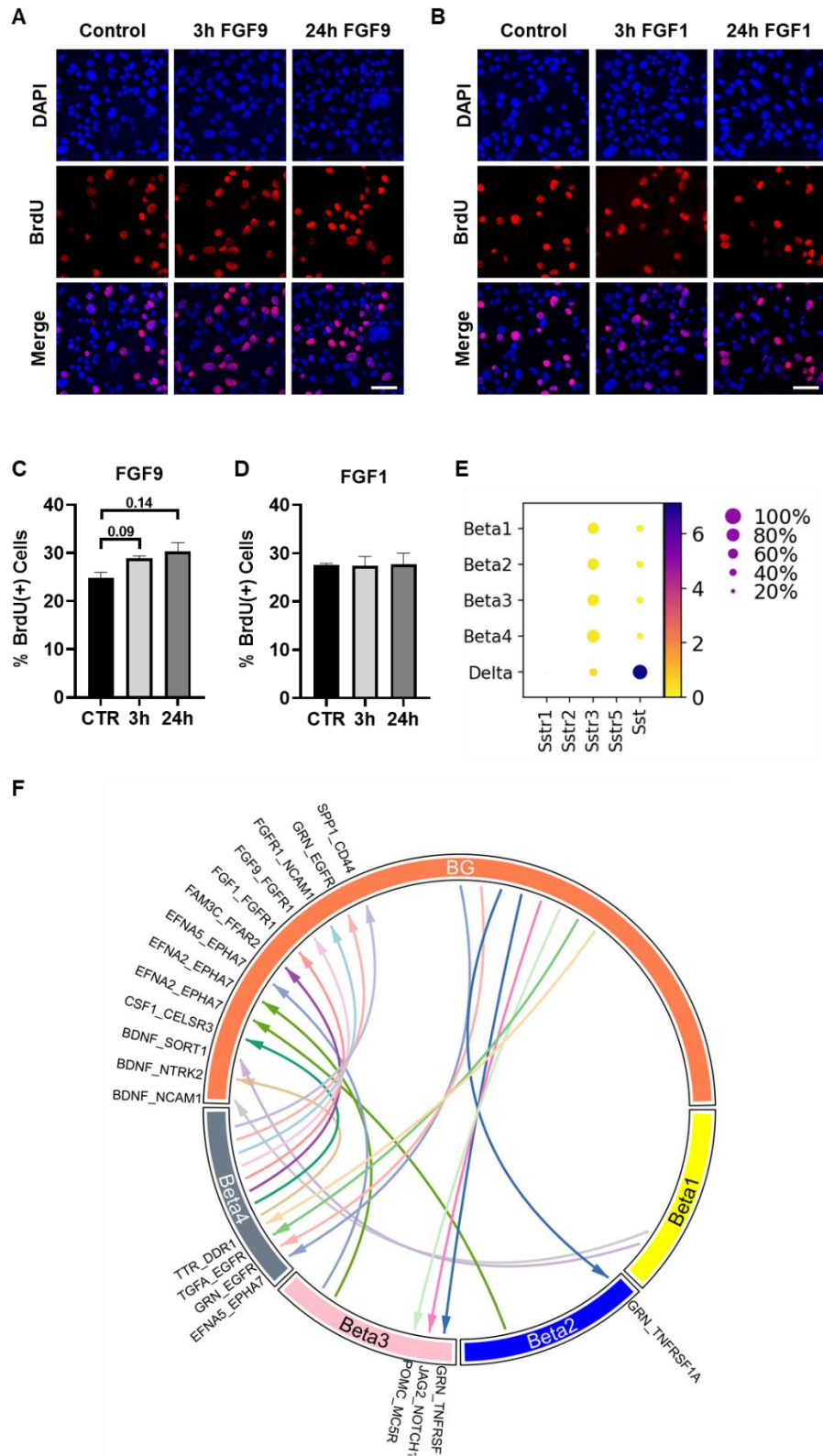
**C**



**Supplemental Figure 8. Identification of unique *Beta4* modules via comparison of DiffCoEx-modules with WGCNA-modules.**

(A) Screening of DiffCoEx-modules (from analysis comparing *Beta1-3* against *Beta4*) for *Beta4*-specific modules. (B, C) Circos plots showing the top 25 differentially co-expressed genes of the *Beta4*-specific modules M6 (B) and M10 (C) in *Beta1-3*. Genes that are co-expressed are connected by a red line. The degree of co-expression is reflected via the thickness of the line (thicker being a higher degree of co-expression).





**Supplemental Figure 9. Cell-cell communication between BG and  $\beta$ -cells.**

(A-D) DAPI- and BrdU-staining of serum-starved MIN6  $\beta$ -cells stimulated with FGF9 (A, C) and FGF1 (B, D) for 3 and 24 hours. (E) Dot plot representing the number of cells (dot size) and mean gene expression levels of the  $\delta$ -cell hormone *Sst* and its receptors (*Sstr1-5*) in the *Beta1-4* and *Delta* clusters. *Sstr4* was not detected. (F) Circle plot depicting potential intercellular communication (based on ligand-receptor gene expression) in dual-hormonal BG cells and  $\beta$ -cell clusters *Beta1-4*. Arrow directions are from ligand to receptor. Non-unique interactions likely to occur between BG cells and all four  $\beta$ -cell clusters are not shown.